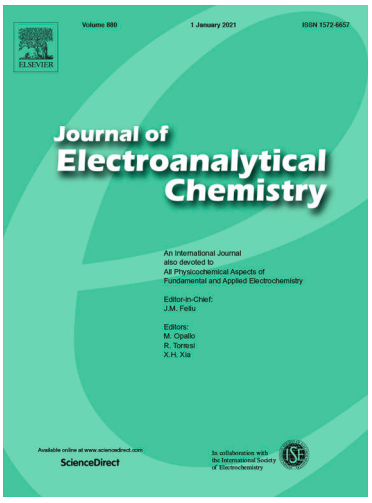

A novel electrochemical sensor for monitoring ovarian cancer tumor protein CA 125 on benzothiophene derivative based electrodes

Omer Faruk Er, Hilal Kivrak, Omruye Ozok, Sebahattin Çelik, Arif Kivrak

PII: S1572-6657(21)00880-8
DOI: https://doi.org/10.1016/j.jelechem.2021.115854
Reference: JEAC 115854

To appear in: *Journal of Electroanalytical Chemistry*

Received Date: 11 July 2021
Revised Date: 2 November 2021
Accepted Date: 5 November 2021

Please cite this article as: O. Faruk Er, H. Kivrak, O. Ozok, S. Çelik, A. Kivrak, A novel electrochemical sensor for monitoring ovarian cancer tumor protein CA 125 on benzothiophene derivative based electrodes, *Journal of Electroanalytical Chemistry* (2021), doi: https://doi.org/10.1016/j.jelechem.2021.115854

A novel electrochemical sensor for monitoring ovarian cancer tumor protein CA 125 on benzothiophene derivative based electrodes

Omer Faruk Er[a], Hilal Kivrak[b,c*], Omruye Ozok[d], Sebahattin Çelik[e], Arif Kivrak[d+]

[a]*Department of Chemical Engineering, Faculty of Engineering, Van Yüzüncü Yil University, Van, 65000, Turkey*

[b]*Translational Medicine Research and Clinical Center, Eskisehir Osmangazi University, 26040 Eskisehir, Turkey*

[c]*Department of Chemical Engineering Faculty of Engineering and Architectural Sciences, Eskisehir Osmangazi University, 26040, Eskişehir Turkey*

[d]*Department of Chemistry, Faculty of Sciences and Arts, Eskisehir Osmangazi University Eskişehir, 26040 Turkey*

[e]*Department of General Surgery, Faculty of Medicine, Van Yüzüncü Yil University, 65000, Van, Turkey*

Corresponding Authors:*e-mail: hilalkivrak@gmail.com, hilaldemir.kivrak@ogu.edu.tr
[+]e-mail: arif.kivrak@ogu.edu.tr

ABSTRACT

COVID-19 crisis affects ovarium cancer patients seriously. Thus, it is vital to diagnose ovarium cancer, one of the most common types of cancer diagnosed and the causes of death of women around the world, at early stages. Herein, 5-(2-phenylbenzo[b]thiophen-3-yl) thiophene-2-carbaldehyde (PTTC)-based sensor is designed to detect CA-125 more precisely and rapidly via electrochemical methods. PTTC, novel benzothiophene derivative, is synthesized by electrophilic cyclization reactions and Pd-catalyst coupling reactions. Then, PTTC is dispersed homogeneously in Nafion solution, and an ink is obtained. This ink is transferred onto the glassy carbon electrode and CA-125 is incubated on this electrode. Cyclic voltammetry (CV), differential pulse voltammetry (DPV), and electrochemical impedance spectroscopy measurements are employed to determine sensitivity and reliability of CA-125 on PTTC based GCE electrode. The effect of CA 125 concentration, incubation time, scan rate studies are performed by CV to determine the optimum conditions. Optimum conditions are found as 3 µL PTTC loading, 5000 ng/mL CA125 antigen concentration and 30 min incubation time. Linear range of the PTTC based GCE electrode prepared at optimum conditions are obtained by DPV as 1- 100 ng/ml.Limit of detection and limit of quantification values were obtained as

0.0096 **ng/mL** and 0.0288 ng/mL, respectively. Interference and artificial serum results reveal that this electrode is a promising electrode for CA125 antigen determination for the ovarium cancer. PTTC is a novel and unique material for the detection of ovarium cancer antigen CA-125 and promising for CA-125 antigen detection.

Keywords: CA 125; ovarian; benzothiophene; sensor; cancer

1. Introduction

Coronavirus, known as the coronavirus pandemic, is continuing its spread across the world, with over 42 million confirmed cases in 189 countries and more than 1.15 million deaths. During coronavirus spread, cancer patients, their families, and healthcare facilities are witnessing unprecedented challenges. Furthermore, COVID-19 crisis has affected ovarium cancer patients care, specifically, in-person office visits, laboratory tests, imaging studies, treatments, and surgeries [1-6]. Thus, recently it is vital to diagnose ovarium cancer at early stages. Ovarian cancer is one of the most common types of cancer diagnosed and the causes of death of women around the world. The most important reason for the high death rate from ovarian cancer is the lack of biological markers that provide an early diagnosis of ovarian cancer [7-10]. Moreover, the most of cases are late diagnosed due to symptoms of ovarian cancer observed late. At the late-stage of ovarian cancer, it becomes incurable in most of the cases [11]. Biological markers or tumor markers are biochemical substances rising their concentration in the presence of cancer. Biological markers are produced by the tumor itself, or produced by the body in the cases such as inflammation [9]. Tumor markers could be DNA, antibody, RNA, peptide, protein structures. Tumor markers can be analyzed in secretions such as whole blood, plasma, serum, saliva, urine, feces, and nipple discharge. Tumor markers are the most important factor that distinguishes a disease-affected person from a person having the disease [12].

Cancer antigen 125 (CA-125) is a biomarker found in ovarian cancer cells and used in the diagnosis of ovarian cancer and monitoring the treatment process. CA-125 or Mucin 16 (MUC16) is a protein found in normal values (0-35 U/mL) in the bloodstream of healthy women. The higher than the normal value range (higher than 35 U/ml) of this protein in the bloodstream is associated with the progression of ovarian cancer. Therefore, the CA-125 test could be used to monitor cancer during and after the treatment of ovarian cancer [13, 14].

The determination of CA-125 concentration in the bloodstream is usually performed by the ELISA method that is an immunoenzymatic colorimetric method. Electrochemical method is due to its low cost, high sensitivity, fast, and time saving to determine and screen the level of CA-125 in the bloodstream for early diagnosis of ovarian cancer. Thus, recent years, researches concentrated on the electrochemical methods for early diagnosis of ovarian cancer [15-23]. LOD, LOQ, and linear range values of various studies compiled from the literature on the determination of CA-125 by electrochemical methods are given in Table 1.

Gazze et al. developed a sensor to diagnose CA-125 via deposition of a polyaniline layer with electro-polymerization on a screen-printed graphene electrode. Then, it was functionalized with the CA-125 antibody via covalent cross-links. Sensor was able to detect CA-125 as low as 0.923 ng/μL over the dynamic range of 0.92 pg/μL-15.2 ng/μL [24]. Wu et al. reported the results of a sensor consisting of soluble carbon nanofiber, CA-125 antigen, thionine for electron transfer, and horseradish peroxidase (HRP). It was found that this sensor had a high sensitivity, repeatability, and good stability with 1.8 U/ml detection limit [25]. Hasanzadeh et al. reported that a sensor capable of detecting CA-125 was developed by depositing cysteamine-capped gold nanoparticles on the surface of reduced graphene oxide (ERGO) probe via electrophoretic deposition method. It was stated that this sensor had direct electron transfer capability and being a low limit of quantification of 0.1 U/mL [26]. Johari-Ahar et al. reported that modified the gold electrode with mercaptopropionic acid (MPS) and then developed a sensor by

conjugating silica-coated gold nanoparticles (AuNPs@SiO2), CdSe quantum dots (QDs), and anti-CA-125 monoclonal antibody, respectively. It was found that this sensor could sensitively detect CA-125 with a low detection limit of 0.0016 U/mL and a linear detection range of 0-0.1 U/mL [27]. Zhang and coworkers reported a detailed review on employment of metal-organic frameworks (MOFs) which also is a ultrasensitive and highly selective biosensors for detection cancer biomarkers [28]. Wang and coworkers also worked on two kinds of bimetallic TbFe-MOFs and utilized them as a platform for CA125 detection and as a result proposed aptasensor based on Tb-MOF-on-Fe-MOF exhibited great potentials for early diagnosis of tumors [29].

Table 1: LOD, LOQ, and Linear range values of electrode materials compiled from literature for electrochemical determination of CA 125.

Ovarian cancer tumor marker	sensor	LOD or LOQ	Linear range	Ref
CA125	MoS_2-gold-nanoflowers	0.36 pg/ml	0.01-50 ng/mL	[30]
CA125	Gold NP-ZnO nanorods	2.5 ng/µL	2.5 ng/µL-1 ng/µL	[31]
CA125	FA-HCl-doped polyaniline-chitosan and Ag-Co_3O_4 nanosheets	0.25 pg/mL	0.001-25 ng/ml	[32]
CA125	Three dimensional gold electrode	1 pg/mL	1 fg/ml-1 µg/ml	[33]
CA125	Graphene polyaniline	0.923 ng/µL	0.92 pg/µL-15.2 ng/µL	[24]
CA125	GO-chitosan-PGMA	0.05 ng/mL	0.05-100 ng/mL	[34]
CA 125	**GCE+Nafion+PTTC antibody**	0.0096 **ng/mL (LOD)** 0.0288 ng/mL **ng/mL (LOQ)**	**0.01-100 ng/mL**	**This work**

Heteroaromatic compounds such as indoles, pyrazoles, benzothiophenes, and carbazols are of great importance in health and in the development of new materials due to their superior properties [35-39]. They are used as drugs such as anticancer, antioxidants, antifungal, antibacterial, anti-parasites, and in applications such as topoisomerase inhibitors, potassium channel openers, and L1210 cell selectors for years [40-47]. Among the heteroaromatic

structures, benzothiophene derivatives are the best known and are used as pharmaceuticals such as raloxifene as used in the treatment of breast cancer and postmenopausal osteoporosis. In addition, they have been used as antitumor, antihypertensive, antimicrobial agents [37, 48]. Therefore, the synthesis of benzothiophene derivatives and the discovery of new properties are of great importance for use in new applications.

Herein, a sensor that can detect CA-125 using a novel benzothiophene derivative has developed. PTTC used in sensor was synthesized via electrophilic cyclization reaction and Pd-catalyst coupling reactions. This sensor was prepared by modification of glassy carbon with PTTC as an antibody against CA-125 antigen.

2. Materials and Methods

Fabrication of the sensor

The glassy carbon electrode was washed with deionized water by glazed with alumina and then it was kept in an ultrasonic bath in 1:1 ethanol and deionized water solution. The electrode was finally dried in the flow of nitrogen gas. An ink was obtained by dispersing 5 mg of PTTC in 1 mL of Nafion; and 3 µl from this ink was transferred on modified-GCE and dried at room temperature. Subsequently, distinct concentrations among 1-50000 ng/ml CA-125 antigens were incubated onto modified-GCE at room temperature for 10-70 minutes.

Electrochemical measurements

Electrochemical measurements for the produced sensor were taken via CV, EIS, and DPV. CV measurements were obtained on produced sensor electrodes at room temperature in PBS (pH: 7.4) + 5 mM $Fe(CN)_6^{3-/4-}$ solution (Scan rate = 50 mV s^{-1}) at 5000 ng/ml CA-125 antigen concentration for GCE, Nafion + GCE, Nafion + PTTC + GCE, Nafion + PTTC + CA-125 + GCE. After the sensor was designed, the surface of electrodes was exposed to distinct concentrations of CA-125 antigen varying among 1-50000 ng/ml. Furthermore, to examine the

impact of CA-125 antigen concentration on the surface of electrode, CV measurements were performed at room temperature in PBS (pH: 7.4) + 5 mM $Fe(CN)_6^{3-/4-}$ solution (scan rate = 50 mV s^{-1}). The best CA-125 antigen concentration range was found as 5000 ng/ml and subsequently, the incubation time on the electrode of the CA-125 antigen was researched at differing times between 10-70 min. To investigate the impact of scan rate on CA-125 antigen in the sensor, CV measurements at different scan rates ranging from 5-1000 mV s^{-1} on the incubated electrode with 5000 ng/ml CA-125 antigen were received in PBS (pH: 7.4) + 5 mM $Fe(CN)_6^{3-/4-}$ solution. In addition, DPV measurements were received on sensor electrode prepared by incubating 5000 ng/ml CA-125 antigen. The sensitivity of the sensor was estimated from the slope of the calibration plot of the DPV curves obtained by drawing the concentration values against the maximum current.

In order to determine the electrooxidation process of the CA-125 antigen in the sensor, EIS measurements at varying potentials were taken on the sensor produced with 3 ml PTTC + 5000 ng/ml CA-125 antigen incubated for 30 minutes.

For the interference measurements of sensor produced, CV measurements were received on sensor fabricated with PTTC + 5000 ng/ml CA-125 antigen incubated for 30 minutes. Interference measurements in the absence and presence of 5000 ng/ml CA-125 antigen were taken in PBS + dopamine (0.1 mM), PBS + uric acid (2.5 mM), PBS + glucose (4.7 mM), PBS + ascorbic acid (0.1 mM), arginin (0.1 mM)+PBS (pH: 7.4), D-L valin(0.1 mM)+PBS (pH: 7.4), glutamin (0.1 mM)+PBS (pH: 7.4), glycin (0.1 mM)+PBS (pH: 7.4), histidine (0.1 mM)+PBS (pH: 7.4), l-asparagin (0.1 mM)+PBS (pH: 7.4), L-methionin (0.1 mM)+PBS (pH: 7.4), leucin (0.1 mM)+PBS (pH: 7.4), prolin (0.1 mM)+PBS (pH: 7.4), serin (0.1 mM)+PBS (pH: 7.4 solutions at room temperature (scan rate = 50 mV s-1).

Moreover, the isotonic serum measurements with 0.9% isotonic sodium chloride and the artificial serum measurements with a solution prepared to contain PBS (pH: 7.4), urea (2.5 mM), (D+)-glucose (4.7 mM), $MgCI_2$ (1.6 mM), KCI (4.5 mM), and $CaCI_2$ (5 mM) were taken via CV and EIS at room temperature.

3. Results and Discussion

5-(2-phenylbenzo[b]thiophen-3-yl) thiophene-2-carbaldehyde (PTTC)	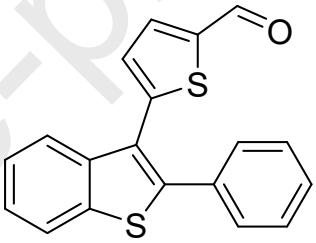

Figure 1: Synthesis of PTTC.

The compound PTTC as an antibody was used to detect CA-125 antigen with electrochemical methods via CV, EIS, and DPV. CV measurements were taken on prepared electrodes modified-GCE, modified-GCE + Nafion, modified-GCE + Nafion + CA-125, modified-GCE + Nafion + PTTC, modified-GCE + Nafion + PTTC + 5000 ng/ml CA-125 (30 min. incubation time) and in PBS (pH: 7.4) + 5.0 mM $Fe(CN)_6^{3-/4-}$ solution at room temperature (scan rate = 50 mV s^{-1}). The results of these CV measurements are given in Figure 2. The peaks of CA-125 antigen in forward scan with 0.124 mA cm^{-2} current density at 0.17 V and in backward scan with 0.117 mA cm^{-2} current density at -0.18 V were obtained (Fig. 2). These values obtained are higher than the values stated in the studies on CA-125 antigen in the literature [15-23].

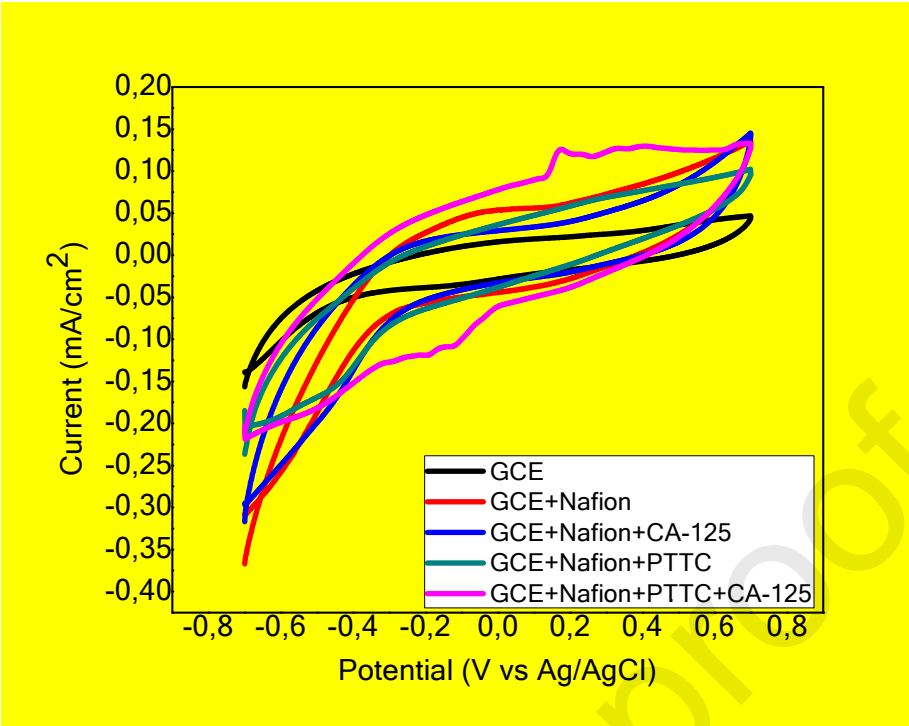

Figure 2: Cyclic voltammograms for modified GCE, Nafion+GCE, Nafion+PTTC+GCE, Nafion+CA-125+GCE and GCE+Nafion+PTTC+CA-125 and at 5000 ng/ml CA-125 antigen concentration.

To examine the concentration effect of CA-125 antigen used in the designed sensor, CV measurements were obtained by incubating amounts of CA-125 antigen varying among 1-50000 ng/ml for 30 min on the GCE + Nafion + PTTC electrode in PBS (pH: 7.4) + 5 mM $Fe(CN)_6^{3-/4-}$ at room temperature (scan rate = 50 mV s^{-1}). CV results are given in Figure 3a-b. It could be note that the current density gradually increases from 1 ng/ml (0.01 mA cm^{-2}) to 5000 ng/ml (0.122 mA cm^{-2}) and the current density decreases after 5000 ng/ml. The results showed that the sensor obtained by incubating 5000 ng/ml CA-125 antigen for 30 minutes had the maximum current density.

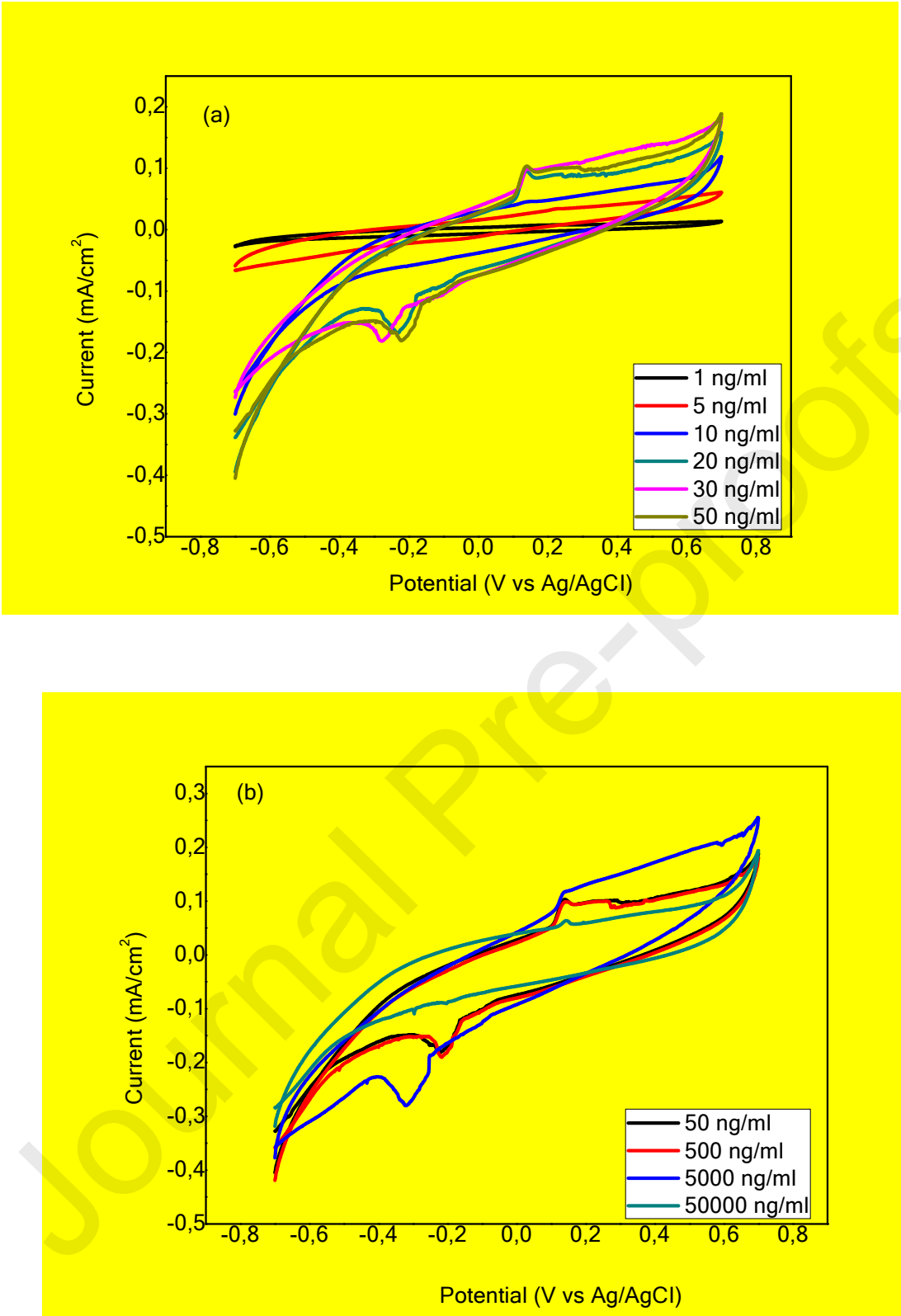

Figure 3: Cyclic voltammograms received on sensor electrode produced with 3 µL PTTC antibody + (a) 1-50 ng/ml and (b) 50-50000 ng/ml CA-125 antigen and at 30 min incubation time

After the best CA-125 antigen concentration was found as 5000 ng/ml, optimum incubation time was researched for the construction sensor over prepared electrodes by varying time between 10-70 min. The CV measurements taken are given in Figure 4a. The results showed that the best incubation time for the sensor was 30 minutes. To research the effect of scan rate on the electrooxidation of CA-125 antigen, CV measurements were taken on electrode prepared with modified-GCE + Nafion + 3 µL PTTC + 5000 ng/ml CA-125 antigen through 30 min incubation time, and these results are given Figure 4b. It was observed that as the scan rate increased, the current density increased. This phenomenon may be explained sensing reaction is controlled via diffusion.

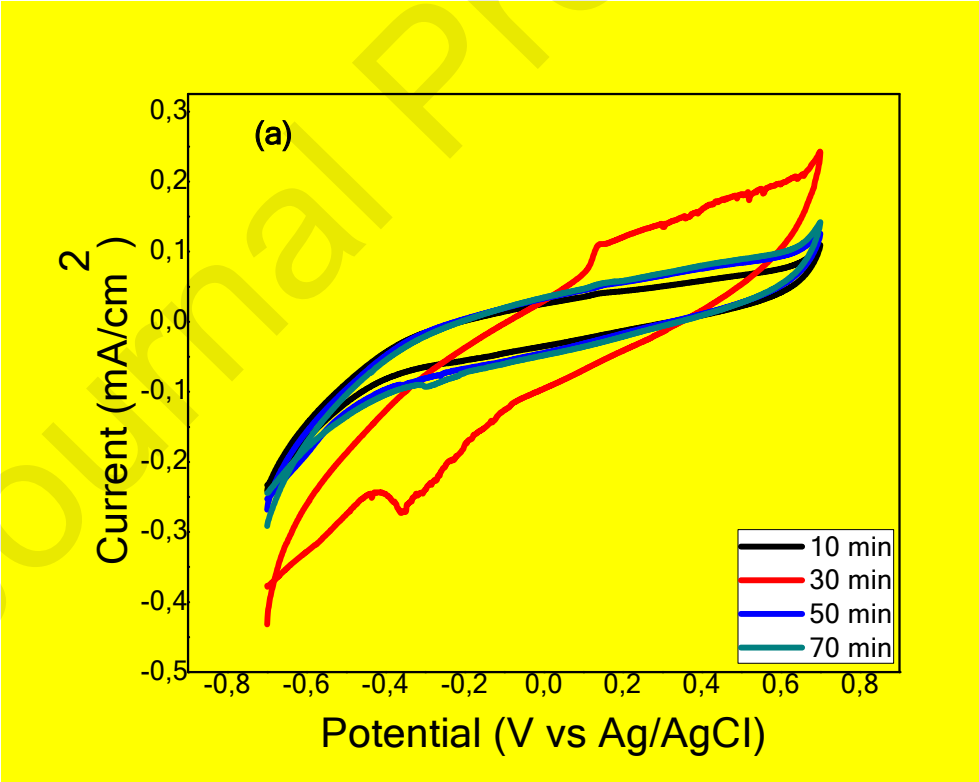

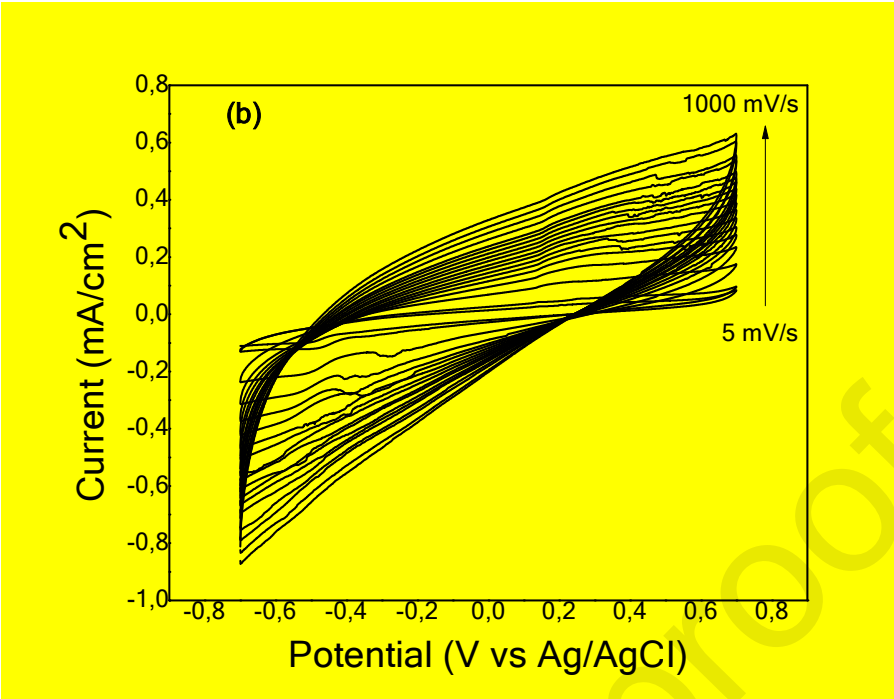

Figure 4: Cyclic voltammograms **a)** received on sensor electrode produced with 3 µL PTTC antibody+5000 ng/ml CA-125 antigen at varying incubation times of 10-70 min in PBS (pH: 7.4) + 5.0 mM $Fe(CN)_6^{3-/4-}$ (scan rate=50 mV s^{-1}), and **b)** received on sensor electrode produced with 3 µL PTTC antibody+5000 ng/ml CA-125 antigen at 30 min incubation time in PBS (pH: 7.4) + 5.0 mM $Fe(CN)_6^{3-/4-}$ at room temperature (scan rate=5-1000 mV s^{-1}).

Sensitivity of the sensor electrode fabricated with 3 µL **PTTC** antibody + various concentration of CA125 antigen at 30 min incubation time was determined by the DPV method in PBS. The DPV curves for these electrodes in 0.1 M PBS at varying concentrations (0.01-1000 ng/mL CA 125 antigen) are depicted in **Figure 5a**. The calibration plot of the DPV peak current densities versus concentration of CA125 antigen is also illustrated in **Figure 5b.** One can note that the DPV current densities versus CA125 antigen concentration plot exhibited a linear relationship within the range of 0.01-100 ng/mL. This linear range value is higher than those reported in the literature (**Table 1**).

Limit of Blank (LOB) and lowest detection limit (LOD) for CA125 antigen measured at acceptable statistical certainty and lowest concentration of analyte called the limit of quantification (LOQ) determined at acceptable sensitivity were calculated for the sensor

electrode fabricated with 3 µL **PTTC** antibody. To determine LOB, 10 blank electrode responses without analyte were taken and then the standard deviation of 10 blank electrode responses and these blank DPV measurements are presented in **Figure 6**. LOB, LOD, and LOQ were found as 0.0086, 0.0096, and 0.0288 ng/mL at (S/N=3), respectively. It is clear that LOD of this sensor is lower than the sensors reported in literature (**Table 1**).

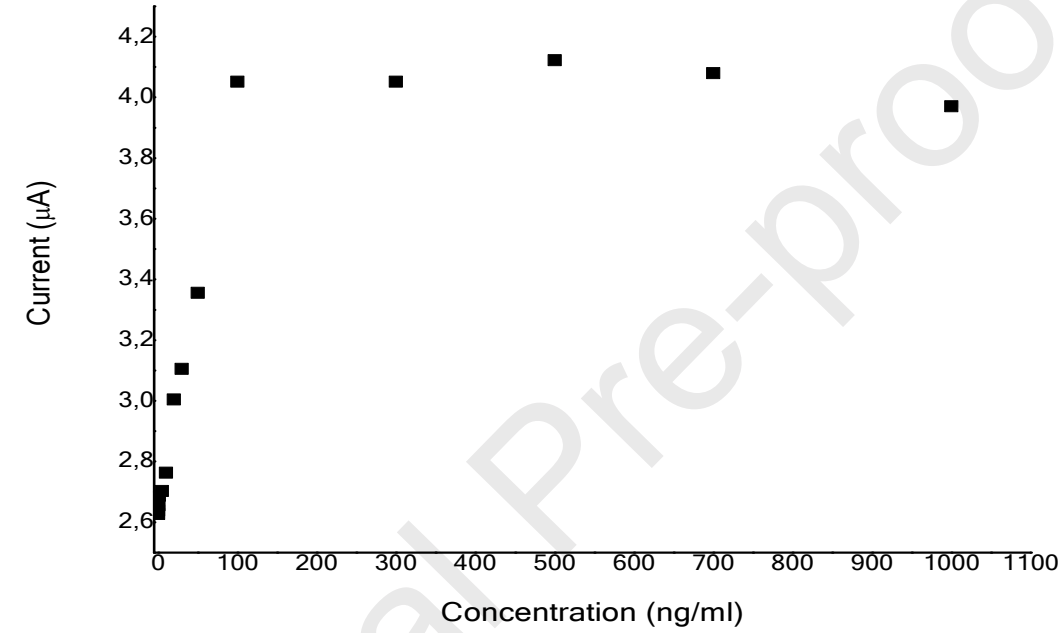

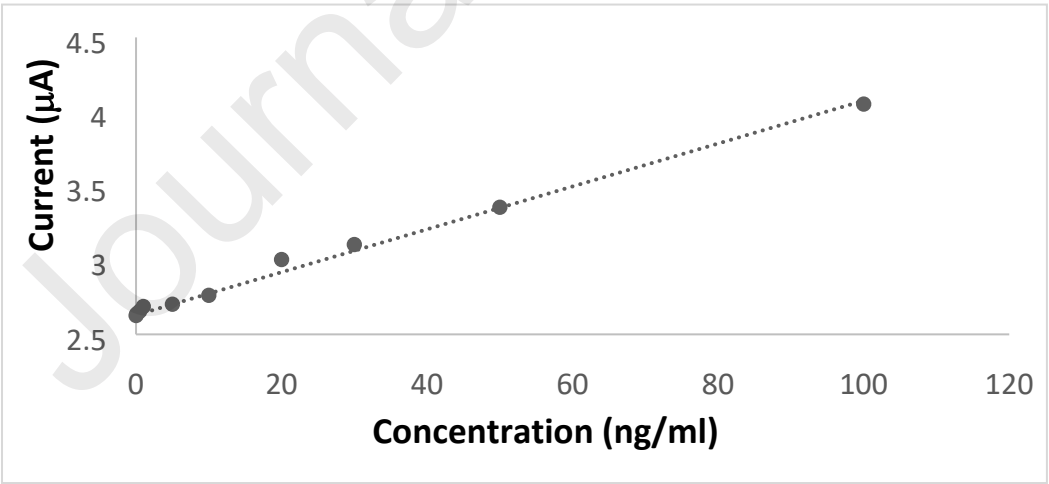

Figure 4: Differential pulse voltammetry measurements received on sensor electrode produced with 3 µL PTTC antibody+0.01-1000 ng/ml CA-125 antigen at room temperature and at 30 min incubation time in PBS + 5.0 mM $Fe(CN)_6^{3-/4-}$.

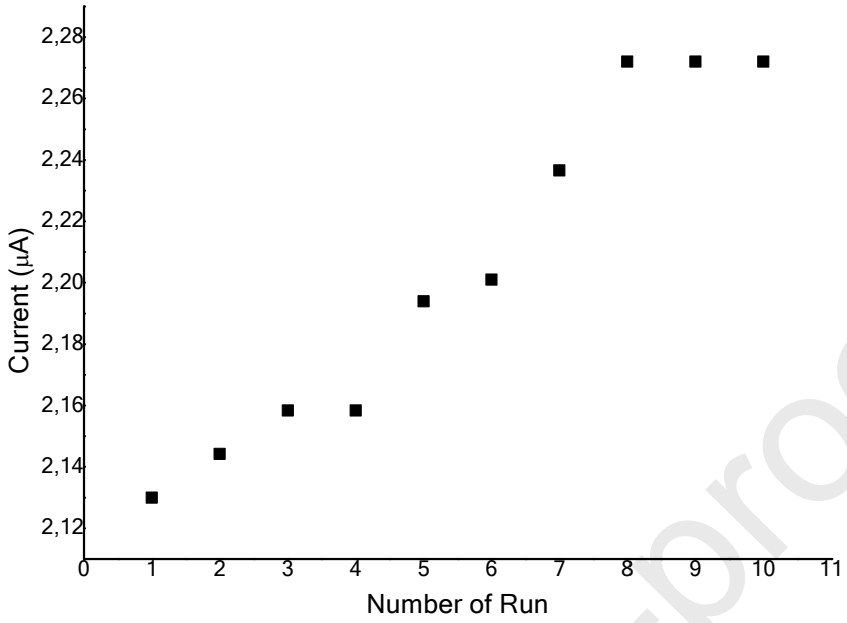

Figure 5: Differential pulse voltammetry measurements received to measure 10 blank electrode responses without analite on sensor electrode produced with 3 μL PTTC antibody in PBS + 5.0 mM $Fe(CN)_6^{3-/4-}$ at room temperature.

Electrochemical impedance spectroscopy is a widely used measurement method in fields such as materials science, electrochemistry, sensors, biology and medicine. Impedance measurement could be defined as the measure of resistance against the current of an alternating current [49]. Nyquist plots obtained from EIS measurements occurs linear parts corresponding to a controlled diffusion process and a semi-circular area that provides information about load transfer. To obtain information about the electrooxidation process of CA-125, EIS measurements were taken on the sensor produced with Nafion+3 μL PTTC+5000 ng/ml CA-125 at varying volts among -0.6-0.6 V in PBS (pH: 7.4) + $Fe(CN)_6^{3-/4-}$ solution. Sensor was produced by incubating 5000 ng/ml of CA-125 antigen for 30 min over GCE + Nafion + PTTC electrode. Nyquist plots obtained from EIS measurements are given in Figure 6. In Nyquist plots, the diameter of the semicircles is associated with the load transfer resistance (Rct), the

larger the diameter, the larger the load transfer resistance, but the smaller the diameter, the lower the load transfer resistance [50]. Herein, it could be explained that when the diameter of the semicircle is large, CA-125 antigen electrooxidation is slow, but when the diameter of the semicircle is small, CA-125 antigen electrooxidation is fast. EIS measurements showed that the diameter of the semicircles was large at potentials between -0.6-0 V, but the diameter of the semi-circles was small at potentials between 0-0.6 V (Fig 5). The lowest charge transfer resistance level for the electrooxidation of CA-125 antigen was found as 0.2 V, and this result is compatible with CV and DPV results [20, 51-58] .

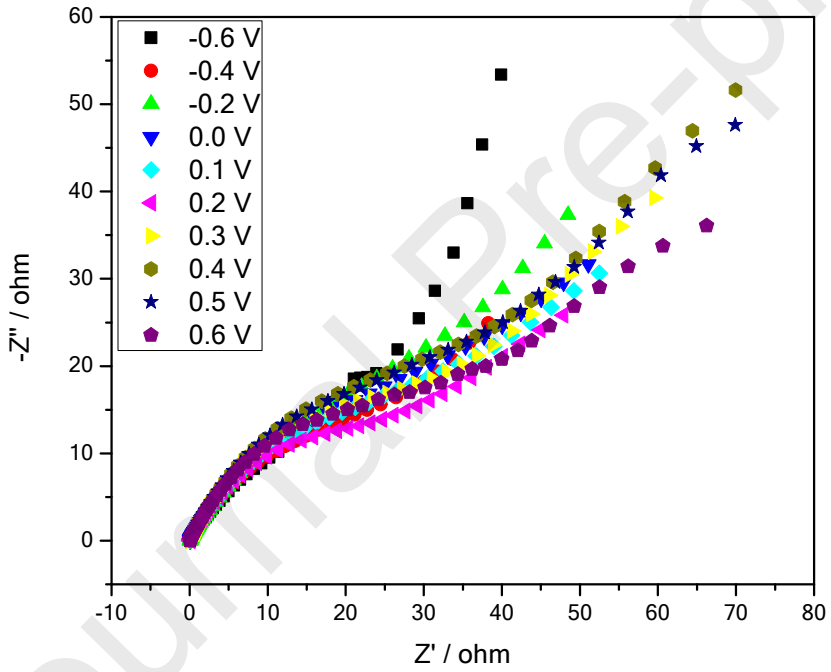

Figure 6: Electrochemical impedance spectra on sensor fabricated with 3 µL PTTC antibody + 5000 ng/ml CA-125 antigen at 30 min incubation time at various potentials in PBS + 5.0 mM $Fe(CN)_6^{3-/4-}$ at frequency range with signal amplitude (10 mV).

Glucose, uric acid, dopamine, and ascorbic acid, arginine, D-L valin, glutamin, glycin, histidine, l-asparagin, L-methionin, leucin, prolin, serin could affect the diagnosis of CA-125 antigen in the blood and urine samples. Thus interference of glucose, uric acid, dopamine, and

ascorbic acid, arginine, D-L valin, glutamin, glycin, histidine, l-asparagin, L-methionin, leucin, prolin, serin was investigated by CV and EIS methods. These interference measurements were taken by CV and EIS at 0.2 V. CV and EIS measurements were performed over sensors fabricated that Nafion+3 µL PTTC electrode, and Nafion+3 µL PTTC+CA-125 by incubating 5000 ng/ml CA-125 antigen for 30 min, respectively. Interference measurements were taken by CV and EIS measurements in D-glucose (4.7 mM)+PBS (pH: 7.4), dopamine (0.1 mM)+PBS (pH: 7.4), uric acid (2.5 mM)+PBS (pH: 7.4), ascorbic acid (0.1 mM)+PBS (pH: 7.4), arginin (0.1 mM)+PBS (pH: 7.4), D-L valin(0.1 mM)+PBS (pH: 7.4), glutamin (0.1 mM)+PBS (pH: 7.4), glycin (0.1 mM)+PBS (pH: 7.4), histidine (0.1 mM)+PBS (pH: 7.4), l-asparagin (0.1 mM)+PBS (pH: 7.4), L-methionin (0.1 mM)+PBS (pH: 7.4), leucin (0.1 mM)+PBS (pH: 7.4), prolin (0.1 mM)+PBS (pH: 7.4), serin (0.1 mM)+PBS (pH: 7.4) solutions at room temperature. CV and EIS measurements of D-glucose (4.7 mM)+PBS (pH: 7.4), dopamine (0.1 mM)+PBS (pH: 7.4), uric acid (2.5 mM)+PBS (pH: 7.4), ascorbic acid (0.1 mM)+PBS (pH: 7.4) are given Figure S1 (a-d) and Figure S2 (a-d), respectively. On the other hand, EIS measurements for arginin (0.1 mM)+PBS (pH: 7.4), D-L valin(0.1 mM)+PBS (pH: 7.4), glutamin (0.1 mM)+PBS (pH: 7.4), glycin (0.1 mM)+PBS (pH: 7.4), histidine (0.1 mM)+PBS (pH: 7.4), l-asparagin (0.1 mM)+PBS (pH: 7.4), L-methionin (0.1 mM)+PBS (pH: 7.4), leucin (0.1 mM)+PBS (pH: 7.4), prolin (0.1 mM)+PBS (pH: 7.4), serin (0.1 mM)+PBS (pH: 7.4) are given Figure S3 (a-j) The comparison of CV results given in Figure S1 (a-d) was examined with the anodic peak currents increase. The interference effect of uric acid was seen to be greater than ascorbic acid, dopamine, and D-glucose. Similarly, comparing the Nyquist plots given in Figure S2 (a-d) is in agreement with the results showing that the sensor incubated with CA-125 antigen had the lowest load transfer resistance. EIS measurements for the amino acids interference given Figure S3 revealed that components that may prevent the diagnosis of CA-125 in the blood samples could be ignored, and its promise has a good selectivity in the

diagnosis of CA-125 antigen of sensor fabricated with PTTC+5000 ng/ml CA-125 antigen at 30 min incubation time.

After determining the sensitivity, interference effects, LOD and LOQ values of the developed sensor, artificial serum, and isotonic serum measurements were taken. These result were presented in Figure 7. Salts contained in artificial serum and isotonic serum could affect antigen-antibody interactions in the sensor. Artificial serum and isotonic serum measurements were performed over developed sensor with PTTC+5000 ng/ml CA-125 antigen at 30 min incubation time, and these results were compared with obtained results in PBS (pH: 7.4) + $Fe(CN)_6^{3-/4-}$ via EIS at 0.2 V (Fig 7). Artificial serum was prepared by dissolving D-glucose (4.7 mM), urea (2.5 mM), KCl (4.5 mM), $CaCl_2$ (5 mM), and $MgCl_2$ (1.6 mM) salts in PBS (pH: 7.4), and 0.9% isotonic sodium chloride infusion water solution (sterile) was used as an isotonic serum (Fig. 7). Results reveal that EIS has similar behavior in the artificial and isotonic serum medium.

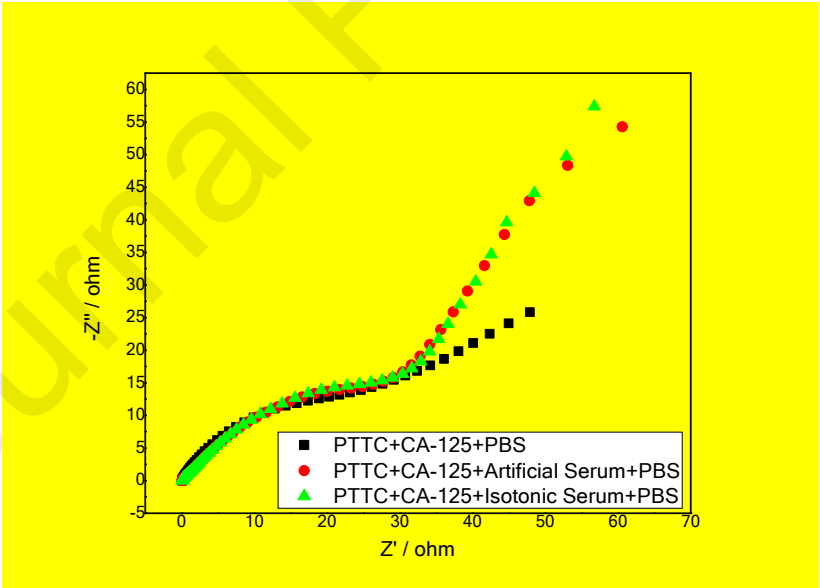

Figure 7: EIS measurements at 0.2 V for comparison with PBS, isotonic serum, and artificial serum on the fabricated sensor consisting of 30 ng/ml CA-125 antigen, 3 µL PTTC antibody, and prepared at 30 min incubation time in PBS + 5.0 mM $Fe(CN)_6^{3-/4-}$ at room temperature.

4. Conclusions

At present, **PTTC** benzothiophene derivative was synthesized to detect CA125 (MUC-16) level via electrochemical methods such as CV, DPV, and EIS. In order to determine the electrochemical parameters affecting sensitivity of the sensor such as CA125 antigen concentration, **PTTC** loading, incubation time, and scan rate were examined. Results reveal that concentration vs maxium peak graph exhibited linear region at 0.01-100 ng/ml. One can note that electrochemical immunosensor fabricated from the PTTC has a wide linear range and superior sensitivity, greater than the literature values reported in the literature. Furthermore LOD, and LOQ were found as 0.0096 **ng/mL (LOD)** and 0.0288 ng/mL **ng/mL (LOQ)** (S/N=3) **respectively.** LOD of this immunosensor is lower than the immunosensors reported in literature. Interference of D-glucose (4.7 mM), dopamine (0.1 mM), uric acid (2.5 mM), ascorbic acid (0.1 mM), arginin (0.1 mM), D-L valin(0.1 mM), glutamin (0.1 mM), glycin (0.1 mM), histidine (0.1 mM), l-asparagin (0.1 mM) L-methionin (0.1 mM), leucin (0.1 mM), prolin (0.1 mM), serin (0.1 mM) were taken by CV and EIS. Interference results reveal that these potential interfering subtances preventing the diagnosis of CA-125 in the blood samples could be ignored. On the other hand, artificial serum and isotinic serum measurements results show that arc diamter for both of the measuremenst are similar and it was found that the artificial serum effect was higher than the isotonic serum. In conclusion, PTTC based GCE electrode is a promising electrode for CA125 antigen determination for the ovarium cancer and it has a potential to be used as an alternative for the diagnosis of ovarium cancer

Acknowledgements

The author (A. Kivrak) would like to acknowledge networking contribution by the COST Action CA17104 “New diagnostic and therapeutic tools against multidrug resistant tumours”.

O. F. Er thank to the council of higher education (YOK) for 100/2000 scholarship and the Scientific and Technological Research Council of Turkey (TUBITAK) for 2211-A scholarship.

References

[1] A. Kivrak, B. Ulas, H. Kivrak, A comparative analysis for anti-viral drugs: Their efficiency against SARS-CoV-2, International Immunopharmacology 90 (2021).
[2] H. Katz, CANCER CARE THROUGH COVID, Psycho-Oncology 30 (2021) 20-21.
[3] A. Caplan, Ethics, cancer, and COVID, Clinical Cancer Research 26(18) (2020).
[4] A.E. Malek, Raad, II, E. Jabbour, Cancer and COVID-19, Lancet 396(10257) (2020) 1066-1067.
[5] D. Moris, D.I. Tsilimigras, D. Schizas, Cancer and COVID-19, Lancet 396(10257) (2020) 1066-1066.
[6] N.E. Sharpless, COVID-19 and cancer, Science 368(6497) (2020) 1290-+.
[7] G.C. Jayson, E.C. Kohn, H.C. Kitchener, J.A. Ledermann, Ovarian cancer, The Lancet 384(9951) (2014) 1376-1388.
[8] B.M. Reid, J.B. Permuth, T.A. Sellers, Epidemiology of ovarian cancer: a review, Cancer biology & medicine 14(1) (2017) 9.
[9] S.N. Han, A. Lotgerink, M.M. Gziri, K. Van Calsteren, M. Hanssens, F. Amant, Physiologic variations of serum tumor markers in gynecological malignancies during pregnancy: a systematic review, BMC medicine 10(1) (2012) 86.
[10] B. Deb, A. Uddin, S. Chakraborty, miRNAs and ovarian cancer: An overview, Journal of cellular physiology 233(5) (2018) 3846-3854.
[11] A.J. Cortez, P. Tudrej, K.A. Kujawa, K.M. Lisowska, Advances in ovarian cancer therapy, Cancer chemotherapy and pharmacology 81(1) (2018) 17-38.
[12] N.L. Henry, D.F. Hayes, Cancer biomarkers, Molecular oncology 6(2) (2012) 140-146.
[13] N. Razmi, M. Hasanzadeh, Current advancement on diagnosis of ovarian cancer using biosensing of CA 125 biomarker: Analytical approaches, TrAC Trends in Analytical Chemistry 108 (2018) 1-12.
[14] T.I. Goonewardene, M.R. Hall, G.J. Rustin, Management of asymptomatic patients on follow-up for ovarian cancer with rising CA-125 concentrations, The lancet oncology 8(9) (2007) 813-821.
[15] T.S. Rebelo, R. Costa, A.T. Brandão, A.F. Silva, M.G.F. Sales, C.M. Pereira, Molecularly imprinted polymer SPE sensor for analysis of CA-125 on serum, Analytica chimica acta 1082 (2019) 126-135.
[16] H.C. Kazici, F. Salman, H.D. Kivrak, Synthesis of Pd–Ni/C bimetallic materials and their application in non-enzymatic hydrogen peroxide detection, Materials Science-Poland 35(3) (2017) 660-666.
[17] N.A. Ertas, E. Kavak, F. Salman, H.C. Kazici, H. Kivrak, A. Kivrak, Synthesis of Ferrocene Based Naphthoquinones and its Application as Novel Non-enzymatic Hydrogen Peroxide, Electroanalysis 32(6) (2020) 1178-1185.
[18] F. Maillard, M. Eikerling, O. Cherstiouk, S. Schreier, E. Savinova, U. Stimming, Size effects on reactivity of Pt nanoparticles in CO monolayer oxidation: The role of surface mobility, Faraday discussions 125 (2004) 357-377.
[19] X. Liang, H. Han, Z. Ma, pH responsive amperometric immunoassay for carcinoma antigen 125 based on hollow polydopamine encapsulating methylene blue, Sensors and Actuators B: Chemical 290 (2019) 625-630.

[20] O. Alal, A. Caglar, H. Kivrak, O. Sahin, Dendrimer Templated Synthesis of Carbon Nanotube Supported PdAu Catalyst and its Application as Hydrogen Peroxide Sensor, Electroanalysis 31(9) (2019) 1646-1655.
[21] L. Wu, J. Chen, D. Du, H. Ju, Electrochemical immunoassay for CA125 based on cellulose acetate stabilized antigen/colloidal gold nanoparticles membrane, Electrochimica Acta 51(7) (2006) 1208-1214.
[22] H. Kivrak, O. Alal, D. Atbas, Efficient and rapid microwave-assisted route to synthesize Pt–MnOx hydrogen peroxide sensor, Electrochimica acta 176 (2015) 497-503.
[23] A. Şenocak, A. Khataee, E. Demirbas, E. Doustkhah, Ultrasensitive detection of rutin antioxidant through a magnetic micro-mesoporous graphitized carbon wrapped Co nanoarchitecture, Sensors and Actuators B: Chemical (2020) 127939.
[24] A. Gazze, R. Ademefun, R.S. Conlan, S.R. Teixeira, Electrochemical impedence spectroscopy enabled CA125 detection; toward early ovarian cancer diagnosis using graphene biosensors, Journal of Interdisciplinary Nanomedicine 3(2) (2018) 82-88.
[25] L. Wu, F. Yan, H. Ju, An amperometric immunosensor for separation-free immunoassay of CA125 based on its covalent immobilization coupled with thionine on carbon nanofiber, Journal of immunological methods 322(1-2) (2007) 12-19.
[26] M. Hasanzadeh, R. Sahmani, E. Solhi, A. Mokhtarzadeh, N. Shadjou, S. Mahboob, Ultrasensitive immunoassay of carcinoma antigen 125 in untreated human plasma samples using gold nanoparticles with flower like morphology: a new platform in early stage diagnosis of ovarian cancer and efficient management, International journal of biological macromolecules 119 (2018) 913-925.
[27] M. Johari-Ahar, M. Rashidi, J. Barar, M. Aghaie, D. Mohammadnejad, A. Ramazani, P. Karami, G. Coukos, Y. Omidi, An ultra-sensitive impedimetric immunosensor for detection of the serum oncomarker CA-125 in ovarian cancer patients, Nanoscale 7(8) (2015) 3768-3779.
[28] S. Zhang, F.L. Rong, C.A.P. Guo, F.H. Duan, L.H. He, M.H. Wang, Z.H. Zhang, M.M. Kang, M. Du, Metal-organic frameworks (MOFs) based electrochemical biosensors for early cancer diagnosis in vitro, Coordination Chemistry Reviews 439 (2021).
[29] M.H. Wang, M.Y. Hu, Z.Z. Li, L.H. He, Y.P. Song, Q.J. Jia, Z.H. Zhang, M. Du, Construction of Tb-MOF-on-Fe-MOF conjugate as a novel platform for ultrasensitive detection of carbohydrate antigen 125 and living cancer cells, Biosensors & Bioelectronics 142 (2019).
[30] X. Wang, W.P. Deng, L. Shen, M. Yan, J.H. Yu, A 3D electrochemical immunodevice based on an Au paper electrode and using Au nanoflowers for amplification, New Journal of Chemistry 40(3) (2016) 2835-2842.
[31] G. Gasparotto, J.P.C. Costa, P.I. Costa, M.A. Zaghete, T. Mazon, Electrochemical immunosensor based on ZnO nanorods-Au nanoparticles nanohybrids for ovarian cancer antigen CA-125 detection, Materials Science & Engineering C-Materials for Biological Applications 76 (2017) 1240-1247.
[32] X. Ren, H. Wang, D. Wu, D.W. Fan, Y. Zhang, B. Du, Q. Wei, Ultrasensitive immunoassay for CA125 detection using acid site compound as signal and enhancer, Talanta 144 (2015) 535-541.
[33] S. Rafique, S. Tabassum, R. Akram, Sensitive competitive label-free electrochemical immunosensor for primal detection of ovarian cancer, Chemical Papers 74(8) (2020) 2591-2603.
[34] Y.F. Wu, P. Xue, K.M. Hui, Y.J. Rang, A paper-based microfluidic electrochemical immunodevice integrated with amplification-by-polymerization for the ultrasensitive multiplexed detection of cancer biomarkers, Biosensors & Bioelectronics 52 (2014) 180-187.

[35] Y. Hieda, M. Anraku, T. Choshi, H. Tomida, H. Fujioka, N. Hatae, O. Hori, J. Hirose, S. Hibino, Antioxidant effects of the highly-substituted carbazole alkaloids and their related carbazoles, Bioorganic & Medicinal Chemistry Letters 24(15) (2014) 3530-3533.
[36] M.-Z. Zhang, Q. Chen, G.-F. Yang, A review on recent developments of indole-containing antiviral agents, European journal of medicinal chemistry 89 (2015) 421-441.
[37] M. Zora, A. Kivrak, C. Yazici, Synthesis of pyrazoles via electrophilic cyclization, The Journal of Organic Chemistry 76(16) (2011) 6726-6742.
[38] A. Kivrak, M. Algso, Design and synthesis of novel thieno-dibenzothiophene derivatives, ABSTRACTS OF PAPERS OF THE AMERICAN CHEMICAL SOCIETY, AMER CHEMICAL SOC 1155 16TH ST, NW, WASHINGTON, DC 20036 USA, 2017.
[39] O. Ozok, E. Kavak, O.F. Er, H. Kivrak, A. Kivrak, Novel benzothiophene based catalyst with enhanced activity for glucose electrooxidation, International Journal of Hydrogen Energy 45(53) (2020) 28706-28715.
[40] A. Rahmouni, S. Souiei, M.A. Belkacem, A. Romdhane, J. Bouajila, H.B. Jannet, Synthesis and biological evaluation of novel pyrazolopyrimidines derivatives as anticancer and anti-5-lipoxygenase agents, Bioorganic Chemistry 66 (2016) 160-168.
[41] D. Richardson, D. Kalinowski, S. Lau, P. Jansson, D. Lovejoy, Cancer cell iron metabolism and the development of potent iron chelators as anti-tumour agents, Biochimica et Biophysica Acta (BBA)-General Subjects 1790(7) (2009) 702-717.
[42] R.B. Pathak, P. Chovatia, H. Parekh, Synthesis, antitubercular and antimicrobial evaluation of 3-(4-chlorophenyl)-4-substituted pyrazole derivatives, Bioorganic & medicinal chemistry letters 22(15) (2012) 5129-5133.
[43] M.M. Shakdofa, M.H. Shtaiwi, N. Morsy, T. Abdel-rassel, Metal complexes of hydrazones and their biological, analytical and catalytic applications: A review, Main Group Chemistry 13(3) (2014) 187-218.
[44] J.C. Coa, W. Castrillón, W. Cardona, M. Carda, V. Ospina, J.A. Muñoz, I.D. Vélez, S.M. Robledo, Synthesis, leishmanicidal, trypanocidal and cytotoxic activity of quinoline-hydrazone hybrids, European journal of medicinal chemistry 101 (2015) 746-753.
[45] Y. Pommier, Topoisomerase I inhibitors: camptothecins and beyond, Nature Reviews Cancer 6(10) (2006) 789-802.
[46] G. Edwards, A.H. Weston, The pharmacology of ATP-sensitive potassium channels, Annual Review of Pharmacology and Toxicology 33(1) (1993) 597-637.
[47] I. Grynyuk, S. Prylutska, D. Franskevych, V. Trush, T. Sliva, M. Slobodyanik, V. Hurmach, Y. Prylutskyy, O. Matyshevska, U. Ritter, Combined action of C60 fullerene with dimethyl-N-(benzoyl) amidophosphate or dimethyl-N-(phenylsulfonyl) amidophosphate on leukemia L1210 cells in silico and in vitro: Die Wirkung von C60-Fulleren mit Dimethyl-N-(benzoyl)-amidophosphat oder Dimethyl-N-(phenylsulfonyl) amidophosphat auf Leukämie-L1210-Zellen in silico und in vitro, Materialwissenschaft und Werkstofftechnik 47(2-3) (2016) 98-104.
[48] M.A. Algso, A. Kivrak, M. Konus, C. Yilmaz, A. Kurt-Kizildoğan, Synthesis and biological evaluation of novel benzothiophene derivatives, Journal of Chemical Sciences 130(9) (2018) 119.
[49] B.-Y. Chang, S.-M. Park, Electrochemical impedance spectroscopy, Annual Review of Analytical Chemistry 3 (2010) 207-229.
[50] O.F. Er, A. Caglar, H. Kivrak, Enhanced electrochemical glucose oxidation in alkaline solution over indium decorated carbon supported palladium nanoparticles, Materials Chemistry and Physics (2020) 123318.
[51] H. Kivrak, K. Selcuk, O.F. Er, N. Aktas, Nanostructured electrochemical cysteine sensor based on carbon nanotube supported Ru, Pd, and Pt catalysts, Materials Chemistry and Physics 267 (2021).

[52] H. Kivrak, K. Selcuk, O.F. Er, N. Aktas, Electrochemical Cysteine Sensor on Novel Ruthenium Based Ternary Catalyst, International Journal of Electrochemical Science 16(5) (2021).
[53] N.A. Ertas, E. Kavak, F. Salman, H.C. Kazici, H. Kivrak, A. Kivrak, Synthesis of Ferrocene Based Naphthoquinones and its Application as Novel Non-enzymatic Hydrogen Peroxide, Electroanalysis 32(6) (2020) 1178-1185.
[54] A. Caglar, H.C. Kazici, D. Alpaslan, Y. Yilmaz, H. Kivrak, N. Aktas, 3-Acrylamidopropyl-trimethylammoniumchloride cationic hydrogel modified graphite electrode and its superior sensitivity to hydrogen peroxide, Fullerenes Nanotubes and Carbon Nanostructures 27(9) (2019) 736-745.
[55] H.D. Kivrak, N. Aktas, A. Caglar, Electrochemical production of Graphene Oxide and its application as a novel Hydrogen Peroxide sensor, International Journal of Nano Dimension 10(3) (2019) 252-259.
[56] H.C. Kazici, A. Caglar, T. Aydogmus, N. Aktas, H. Kivrak, Microstructured prealloyed Titanium-Nickel powder as a novel nonenzymatic hydrogen peroxide sensor, Journal of Colloid and Interface Science 530 (2018) 353-360.
[57] O. Sahin, H. Kivrak, A. Kivrak, H.C. Kazici, O. Alal, D. Atbas, Facile and Rapid Synthesis of Microwave Assisted Pd Nanoparticles as Non-Enzymatic Hydrogen Peroxide Sensor International Journal of Electrochemical Science 13(2) (2018) 2186-2192.
[58] H. Kivrak, O. Alal, D. Atbas, Efficient and rapid microwave-assisted route to synthesize Pt-MnOx hydrogen peroxide sensor, Electrochimica Acta 176 (2015) 497-503.